# Average Modeling and Nonlinear Observer Design For Pneumatic Actuators With On/Off Solenoid Valves

Khaled Laib, Minh Tu Pham, Xuefang Lin-Shi, Redha Meghnous

# Average modeling and Nonlinear Observer Design For Pneumatic Actuators With On/Off Solenoid Valves

**Khaled Laib, Minh Tu Pham, Xuefang Lin-Shi and Ahmed Redha Meghnous**

Univ Lyon, INSA Lyon, Université Claude Bernard Lyon 1, Ecole Centrale de Lyon, CNRS, Ampère, UMR5005,

69621 Villeurbanne, France

Email: khaled.laib.x060230@gmail.com, <minh-tu.pham,xuefang.lin-shi>@insa-lyon.fr

*This paper presents an averaged state model and the design of nonlinear observers for an on/off pneumatic actuator. The actuator is composed of two chambers and four on/off solenoid valves. The elaborated averaged state model has the advantage of using only one continuous input instead of four binary inputs. Based on this new model, a high-gain observer and a sliding-mode observer are designed using the actuator position and the pressure measurements in one of the chambers. Finally, their closed-loop performances are verified and compared on an experimental benchmark.*

## 1 INTRODUCTION

Pneumatic actuators are widely used in the automation of different industrial production lines, robotics and medical applications. These systems present many advantages: reliability, velocity, low cost and effort/input energy ratio, which allow building light and powerful actuators. Depending on the technique used to deliver and to extract compressed air from the pneumatic chambers, we can distinguish two types of pneumatic actuators: actuators with servo-valves and actuators with on/off solenoid valves. The first type of pneumatic actuators can deliver an airflow rate, depending on the control voltage and the upstream pressure, ranging from $0\%$ to $100\%$. The second type of pneumatic actuators are only able to deliver either $0\%$ or $100\%$ of the available mass flow depending on the binary input voltage of the valves. We focus in this paper on this second type: pneumatic actuators with on/off solenoid valves. The dynamics of pneumatic actuators are nonlinear due mainly to the air compressibility and the behavior of the airflow rate through the components delivering compressed air to the chambers (servo-valves or on/off solenoid valves). In addition to that, actuators with on/off solenoid valves present other fundamental challenges. From an operating point of view and due to their binary inputs, the pneumatic actuators equipped with on/off solenoid valves belong to the class of switched systems with nonlinear dynamics.

In contrast to the rich literature and different control techniques of pneumatic actuators with servo-valves, see for instance [1–6], the literature on pneumatic actuators equipped with on/off solenoid valves remains limited due to the challenges mentioned earlier. The control of these systems was traditionally carried out using hybrid and sequential control, see for instance [7, 8] and the references within. However, from a theoretical point of view, there is no general theory able to characterize the stability of these switched systems in the general case using those approaches.

The recent development of high frequency switching on/off valves has open new perspectives in terms of modeling and control of switched pneumatic actuators. For instance, by considering that the fast on/off valves are similar, from an operating point of view to electric switches, we can use the rich literature of power converters. In power electronics, the concept of switching systems with discrete inputs is well known and averaging techniques are widely used to model power converters. Averaging techniques are used to create one unique model with one continuous input called duty cycle. The control design is then carried out using this new continuous model. Once the continuous input is obtained (as an output of a designed controller), it is converted to discrete inputs (1 or 0) by using a Pulse Width Modulation (PWM) to control

the switched system.

In pneumatic actuators with on/off solenoid valves systems, the valves are controlled with a PWM controller to determine their state: open or close. The average modeling techniques can be used to characterize the equivalent continuous dynamics of the nonlinear system. For instance, the authors of [9] proposed a linear controller based on loop shaping techniques to control the position of the piston. Sliding mode control (see [10–14]) has also been considered as a promising control strategy for pneumatic systems due to its ability to account for the system nonlinearities as well as its dynamic uncertainties. The authors of [15–19] use averaging techniques to derive a nonlinear model which they use to design sliding-mode controllers to control the actuator position.

The different control strategies presented so far require the measurement of all the state variables (position, velocity and pressures of the two chambers) and four sensors are required to implement the previous control strategies. To reduce the implementation costs, we are interested in designing observers to estimate the state variables and hence reducing the number of sensors. In the literature of pneumatic systems with on/off solenoid valves, observer design has been considered in automotive applications and precisely in the control of clutch systems. The authors of [20] propose a reduced-order observer to estimate the pressure which is used afterwards to control the clutch position using an internal pressure controller. In [21], the authors consider the design of a switched observer for an electro-pneumatic clutch actuator with a position sensor. This observer is used in [22] to obtain a dual mode switched controller for the clutch actuator position.

We consider in this paper the derivation of an averaged model, for pneumatic systems with on/off valves, which will be suitable for an easy stability analysis, control and observer designs. Within these objectives, the different previous results suffer from several limitations.

- In modeling and control design: the models of [9, 15–19] are output averaged models. In other words, they are partially averaged model as only the actuator position is averaged while the two pressures are still governed by switched dynamics. Therefore, the existing averaged models have two parts: continuous and switched. This will not allow the elaboration of controllers and observers with simple proofs without requiring tools from hybrid system and sequential control theory.
- In observer design: the observers designed in [20–22] use reduced-order models and have switching dynamics due to the binary inputs of the on/off solenoid valves. As it was mentioned earlier, there is no general theory to guarantee the stability of switched systems in the general case. Therefore, some extra conditions are required to derive stability proofs. For instance, the authors of [21, 22] require a persistence assumption on the velocity signal (persistently exciting condition) for their observation error stability proofs to hold.

**Paper contributions**

We extend our previous results presented in [23] where a full-state averaged model to describe the on/off pneumatic system behavior was elaborated. Our contributions can be summarized as follows.

1. *Averaged Model Validity:* A validity analysis of the on/off pneumatic system full-state averaged model is performed by defining an appropriate criterion and using a well-chosen signal.
2. *Position Control design:* A nonlinear sliding-mode controller is designed based on the full-state averaged model. Conditions on the different control gains are derived to ensure the asymptotic convergence of the tracking errors.
3. *Nonlinear observer design:* The design of nonlinear observers (high gain and sliding modes) using the obtained state averaged model with two outputs. Conditions on the different observer gains are derived to ensure the convergence of the observation errors.
4. *Experimental Validation:* The performance of the proposed nonlinear observers in closed-loop with the designed sliding-mode controller is validated experimentally on a dedicated benchmark.

**Paper outline**

The remainder of this paper is as follows. Section 2 presents the modeling of a pneumatic actuator with four on/off solenoid valves together with the paper objectives. Section 3 presents the principles of average modeling with an illustrative example from power electronics. Those principles are adjusted and used in Section 4 to derive a full-state averaged model of the switched pneumatic actuator and validity analysis of this new model is presented. A robust sliding-mode controller is designed in Section 5 to control the actuator position. Section 6 presents the design of a high-gain observer and a sliding-mode observer. The performances of these observers in closed-loop with the designed sliding-mode controller are verified experimentally in Section 7 with performance comparison. Conclusions and perspectives are drawn in Section 8.

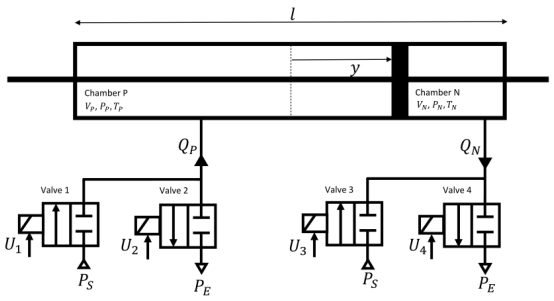


Fig. 1. Pneumatic actuator benchmark

## 2 MODELING AND PROBLEM FORMULATION

We consider a pneumatic actuator with one degree of freedom composed of two pneumatic chambers as illustrated in Fig. 1. Each chamber is connected to a pressure source and an exhaust pressure using two on/off solenoid valves. Each valve $i$ is controlled with a discrete binary input $U_i$.

To model the airflow dynamics in a cylinder, we adopt the following assumptions usually considered in the literature of pneumatic systems and fluid power systems.

- The air is a perfect gas, and its kinetic energy is negligible in each chamber.
- The pressure, the temperature and the density of the air are homogeneous in each chamber.
- The evolution of the air inside each chamber is polytropic.
- The supply and the exhaust pressures are constant.

The complete modeling can be divided into three parts: piston dynamics, air dynamics in each chamber and valves dynamics. Using Newton's second law and the first principle of thermodynamics, the piston dynamics and the air evolution inside each pneumatic chamber are given by [9, 15, 16, 19]

$$\begin{cases} m\ddot{y} = (A_P P_P - A_N P_N) - b_v \dot{y} + f_{ext} \\ \dot{P}_P = \dfrac{k}{(l/2+y)A_P}(rTQ_P - A_P P_P \dot{y}) \\ \dot{P}_N = \dfrac{k}{(l/2-y)A_N}(rTQ_N + A_N P_N \dot{y}) \end{cases} \quad (1)$$

where $l$ is the total length of the pneumatic chamber, $m$ is the mass of the piston and the load connected to it and $b_v$ is the viscosity coefficient. $y$ is the piston position and $f_{ext}$ is the disturbance force. $P_P$, $A_P$ and $Q_P$ (respectively $P_N$, $A_N$ and $Q_N$) are the air pressure, the cylinder area and the input mass-flow rate in chamber $P$ (respectively chamber $N$). $r$ is the perfect gas constant and $k$ is the polytropic constant. $T$ is the air temperature.

$Q_P$ and $Q_N$ are the input mass-flow rates in each chamber and are given by

$$\begin{cases} Q_P = U_1 Q(P_S, P_P) - U_2 Q(P_P, P_E) \\ Q_N = U_3 Q(P_S, P_N) - U_4 Q(P_N, P_E) \end{cases} \quad (2)$$

where $U_i$ with $i = \{1, 2, 3, 4\}$ is the binary input voltage of each valve $i$. The pressures $P_S$ and $P_E$ are the supply and the exhaust pressures, respectively.

The air flow inside each valve depends on the upstream pressure ($P_u$) and temperature ($T_u$); and on the downstream pressure ($P_d$) and temperature ($T_d$). The air flow inside each valve depends also on the valve characteristics such as the mass-flow rate constant $C_{val}$ and the critical pressure ratio $b_{crit}$. The air flow is given by

$$Q(P_u, P_d) = C_{val} P_u \sqrt{T/T_u} \ \times \ldots$$
$$\ldots \times \begin{cases} \sqrt{1 - \left( \dfrac{\frac{P_d}{P_u} - b_{crit}}{1 - b_{crit}} \right)^2} & \text{if } \dfrac{P_d}{P_u} > b_{crit} \\ 1 & \text{if } \dfrac{P_d}{P_u} \leq b_{crit} \end{cases} \quad (3)$$

Note that the external disturbance $f_{ext}$ represents non-measurable forces affecting the piston dynamics. Subsequently in this paper, the term $f_{ext}$ will be dropped from $\ddot{y}$ to have a design model with full parametric knowledge[1]. Thereafter, the global model of Eqn. (1) becomes

$$\begin{cases} \ddot{y} = \dfrac{1}{m}(A_P P_P - A_N P_N - b_v \dot{y}) \\ \dot{P}_P = krT \dfrac{U_1 Q(P_S, P_P) - U_2 Q(P_P, P_E)}{(l/2+y)A_P} - \ldots \\ \qquad \ldots - k\dfrac{P_P}{l/2+y}\dot{y} \\ \dot{P}_N = krT \dfrac{U_3 Q(P_S, P_N) - U_4 Q(P_N, P_E)}{(l/2-y)A_N} + \ldots \\ \qquad +k\dfrac{P_N}{l/2-y}\dot{y} \end{cases} \quad (4)$$

Each binary input voltage $U_i$ can have two physical states either "on" or "off" and every chamber can be in one of the following three states.

- Pressurizing: connected to the supply pressure (for the chamber $P$: $U_1 = 1, U_2 = 0$);

[1] Note that the obtained model will be used to design controllers and observers with robustness properties which will consider neglected and non-modelled dynamics such as $f_{ext}$.

Table 1. The nine operating modes of the pneumatic actuator

| | $M_1$ | $M_2$ | $M_3$ | $M_4$ | $M_5$ | $M_6$ | $M_7$ | $M_8$ | $M_9$ |
|---|---|---|---|---|---|---|---|---|---|
| $U_1$ | 0 | 1 | 0 | 0 | 0 | 1 | 0 | 1 | 0 |
| $U_2$ | 0 | 0 | 1 | 0 | 0 | 0 | 1 | 0 | 1 |
| $U_3$ | 0 | 0 | 0 | 1 | 0 | 0 | 1 | 1 | 0 |
| $U_4$ | 0 | 0 | 0 | 0 | 1 | 1 | 0 | 0 | 1 |

- Venting: connected to the exhaust pressure (for the chamber $P$: $U_1 = 0, U_2 = 1$);
- Close: both of the valves are closed (for the chamber $P$: $U_1 = 0, U_2 = 0$).

From these three states and depending on the input vector $U = (U_1\ U_2\ U_3\ U_4)^T$, nine modes can be obtained for the two chambers as shown in Table 1. However, modes 8 and 9 are functionally redundant since the actuator will not be able to move as there is no pressure difference between chamber $P$ and chamber $N$. Therefore, only modes 1 to 7 are kept in the sequel of this paper. For each of these modes, we define $U_{M_j}$ as

$$\begin{aligned}
&\bullet \text{ Mode 1: } U_{M_1} = (0\ 0\ 0\ 0)^T \\
&\bullet \text{ Mode 2: } U_{M_2} = (1\ 0\ 0\ 0)^T \\
&\bullet \text{ Mode 3: } U_{M_3} = (0\ 1\ 0\ 0)^T \\
&\bullet \text{ Mode 4: } U_{M_4} = (0\ 0\ 1\ 0)^T \\
&\bullet \text{ Mode 5: } U_{M_5} = (0\ 0\ 0\ 1)^T \\
&\bullet \text{ Mode 6: } U_{M_6} = (1\ 0\ 0\ 1)^T \\
&\bullet \text{ Mode 7: } U_{M_7} = (0\ 1\ 1\ 0)^T
\end{aligned} \tag{5}$$

**Problem statement**

Let the pneumatic actuator of Eqn.(4) with four binary inputs $U_1$, $U_2$, $U_3$ and $U_4$ operating with the seven modes given by Eqn. (5), the objectives of this paper are summarized as follows.

- Derive an equivalent model (with one continuous input) able to represent the behavior of the switched system (4);
- Given a desired piston position $y_d$ and using the obtained continuous model, design an observer-based controller and determine the conditions ensuring the convergence of tracking and observation errors.

## 3 AVERAGED MODELING IN POWER ELECTRONICS

In power converter literature where the models have switching dynamics, averaging techniques are used to create one unique model with one single continuous input. By evaluating all the different $p$ modes of a switched system within a PWM period, average modeling consists in merging all these modes resulting in a model where the PWM duty cycle will act as the continuous input.

Consider a switching system with $p$ modes such that

$$\begin{cases} \dot{X} = F_{M_j}(X) \\ W = H_{M_j}(X) \end{cases} \qquad j = 1, \ldots, p$$

where $X$ is the state vector, $F_{M_j}$ and $H_{M_j}$ are the dynamics and the state-output mapping of mode $j$. Note that in each of the previous modes, the switching input is constant and hence the notations $F_{M_j}(X)$ and $H_{M_j}(X)$ instead of the usual notations $F_{M_j}(X, U)$ and $H_{M_j}(X, U)$.

Due to the input variations within a PWM period, the system can switch between several modes. A duty ratio $d_{M_j}$ is associated to each mode $j$. Note that each $d_{M_j}$ is normalized with respect to the total duration of the PWM period and the different $d_{M_j}$ satisfy $\sum_{j=1}^{p} d_{M_j} = 1$.

The averaged model will represent all the $F_{M_j}(X)$ and $H_{M_j}(X)$ within a switching period and the averaged model is given by

$$\begin{cases} \dot{X}_a = \displaystyle\sum_{j=1}^{p} d_{M_j} F_{M_j}(X_a) \\ W_a = \displaystyle\sum_{j=1}^{p} d_{M_j} H_{M_j}(X_a) \end{cases} \tag{6}$$

where $X_a$ and $W_a$ represent the averaged state vector and the averaged output vector, respectively.

**Remark 1.** *At a first glance, one may link Eqn.* (6) *to the T-S fuzzy modeling [24, 25]. However, the average modeling and T-S modeling are fundamentally different. The T-S modeling does not require the mathematical modeling of the system. Instead, the T-S modeling approximates this system by an interpolation of several local linear models (obtained by using simple input-output rules) and combines them using activation functions. Therefore, the T-S modeling can be seen as creating and combing artificial modes to approximate the nonlinear behavior of the system. However, as this technique does not take advantage of the mathematical models, the relevance of the resulting model depends on its ability to represent the actual nonlinear system which is a limitation of the T-S modeling. This is fundamentally different from averaging techniques used in this paper which will reflect the nonlinear behavior. Averaging techniques use the mathematical modeling of the different modes of the nonlinear system.*

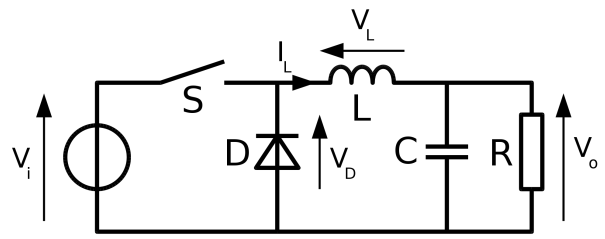


Fig. 2. Buck converter

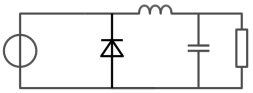

Fig. 3. Mode 1 : buck converter with a closed switch

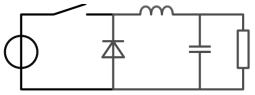

Fig. 4. Mode 2 : buck converter with an open switch

*Then, these modes are combined together to obtain one single model averaging all the modes.*

*Example*

To illustrate the average modeling, we consider the buck converter. Fig. 2 shows a buck converter and its components: a capacitance and an inductor controlled with a single switch and a diode. Depending on the position of the switch, two modes could be considered.

- Mode 1 (Fig. 3): The switch is closed. The diode is reverse biased by $V_i$ and no current is passing through. The voltage across the inductor is $V_L = V_i - V_o$ and the current $I_L$ inside the inductor is increasing.
- Mode 2 (Fig. 4): The switch is open. The diode is forward biased. The voltage across the inductor is $V_L = -V_o$ and the current $I_L$ is decreasing.

Let us consider $I_L$ and $V_o$ as the state variables $X = (I_L \ V_o)^T$ while we consider $V_i$ as the input and $V_o$ as the output (denoted $W$). The dynamics of each mode can be written as

- Mode 1
$$\begin{cases} \dot{X} = \underbrace{\begin{pmatrix} 0 & -\frac{1}{L} \\ \frac{1}{C} & -\frac{1}{CR} \end{pmatrix}}_{A_1} X + \underbrace{\begin{pmatrix} \frac{1}{L} \\ 0 \end{pmatrix}}_{B_1} V_i \\ W = \underbrace{\begin{pmatrix} 0 & 1 \end{pmatrix}}_{C_1} X + \underbrace{\begin{pmatrix} 0 \\ 0 \end{pmatrix}}_{D_1} V_i \end{cases}$$

- Mode 2
$$\begin{cases} \dot{X} = \underbrace{\begin{pmatrix} 0 & -\frac{1}{L} \\ \frac{1}{C} & -\frac{1}{CR} \end{pmatrix}}_{A_2} X + \underbrace{\begin{pmatrix} 0 \\ 0 \end{pmatrix}}_{B_2} V_i \\ W = \underbrace{\begin{pmatrix} 0 & 1 \end{pmatrix}}_{C_2} X + \underbrace{\begin{pmatrix} 0 \\ 0 \end{pmatrix}}_{D_2} V_i \end{cases}$$

In order to obtain an averaged state model, we define $d_{M_1}$ and $d_{M_2}$ as the duty ratios associated to mode 1 and mode 2, respectively. Then, the averaged state model is given by

$$\begin{cases} \dot{X}_a = \sum_{j=1}^{2} d_{M_j} \left( A_j X_a + B_j V_i \right) \\ W_a = \sum_{j=1}^{2} d_{M_j} \left( C_j X_a + D_j V_i \right) \end{cases} \tag{7}$$

where $X_a$ is the averaged state variable vector and $W_a$ is the averaged output. This averaged state model has two inputs $d_{M_1}$ and $d_{M_2}$ satisfying $d_{M_1} + d_{M_2} = 1$. Hence, by choosing $d = d_{M_1}$, then $d_{M_2} = 1 - d$ and the averaged model of Eqn. (7) rewrites after some rearrangements as

$$\begin{cases} \dot{X}_a = \underbrace{\begin{pmatrix} 0 & -\frac{1}{L} \\ \frac{1}{C} & -\frac{1}{CR} \end{pmatrix}}_{A_a} X_a + \underbrace{\begin{pmatrix} \frac{V_i}{L} \\ 0 \end{pmatrix}}_{B_a} d \\ W_a = \underbrace{\begin{pmatrix} 0 & 1 \end{pmatrix}}_{C_a} X_a + \underbrace{\begin{pmatrix} 0 \\ 0 \end{pmatrix}}_{D_a} d \end{cases} \tag{8}$$

This model has one continuous input $d$ and is suitable for simple control strategies since we do not have to deal with any binary inputs. Once the controller is designed and implemented, the input $d$ can be computed and a PWM technique can be used to determine the state (open or closed) of the switch.

## 4 PNEUMATIC ACTUATOR AVERAGE MODELING AND ANALYSIS

We present in this section the derivation of the state averaged model for the pneumatic actuators of Eqn. (4). Then, we analyze the accuracy of this new model compared to the switched model of Eqn. (4).

### 4.1 Pneumatic actuator state averaged model

In the model presented in Eqn. (4), the pressure dynamics $\dot{P}_P$ and $\dot{P}_N$ depend explicitly on the binary discrete inputs $U_i$. Meanwhile, the piston dynamic $\ddot{y}$ depends implicitly on $U_i$ through the pressures $P_P$ and $P_N$.

We can apply averaging techniques, as described in the previous section, on the two pressure dynamics $\dot{P}_P$ and $\dot{P}_N$. However, the resulting model will be a partial averaged state model since the piston dynamics $\ddot{y}$ are not directly averaged. Therefore, to obtain a full averaged state model for the pneumatic actuator, the translation dynamic must depend explicitly on the binary discrete inputs $U_i$.

After introducing the third-order derivative of the position $y$, the model of Eqn. (4) becomes

$$\begin{cases} \dddot{y} = -\dfrac{k}{m}\left(\dfrac{A_P P_P}{l/2+y} + \dfrac{A_N P_N}{l/2-y}\right)\dot{y} - \dfrac{b_v}{m}\ddot{y} + \dots \\ \quad \dots + \dfrac{krT}{m}\dfrac{U_1 Q(P_S,P_P) - U_2 Q(P_P,P_E)}{(l/2+y)} - \dots \\ \quad \dots - \dfrac{krT}{m}\dfrac{U_3 Q(P_S,P_N) - U_4 Q(P_N,P_E)}{(l/2-y)} \\ \dot{P}_P = krT\dfrac{U_1 Q(P_S,P_P) - U_2 Q(P_P,P_E)}{(l/2+y)A_P} - \dots \\ \quad \dots - k\dfrac{P_P}{l/2+y}\dot{y} \end{cases} \tag{9}$$

with $P_N = \dfrac{A_P P_P - m\ddot{y} - b_v\dot{y}}{A_N}$.

As it can be seen in Eqn. (9), the dynamics $\dddot{y}$ and $\dot{P}_P$ change according to the input $U_{M_j}$ of Eqn. (5). Using the following notations

$$X = \begin{pmatrix} x_1 \\ x_2 \\ x_3 \\ x_4 \end{pmatrix} = \begin{pmatrix} y \\ \dot{y} \\ \ddot{y} \\ P_P \end{pmatrix}, \quad F_{M_j}(X) = \begin{pmatrix} f_1 \\ f_2 \\ f_{3_{M_j}} \\ f_{4_{M_j}} \end{pmatrix} = \begin{pmatrix} x_2 \\ x_3 \\ \dddot{y}|_{U_{M_j}} \\ \dot{P}_P|_{U_{M_j}} \end{pmatrix}$$

where the dynamics $f_{3_{M_j}}$ and $f_{4_{M_j}}$ correspond to the dynamics $\dddot{y}$ and $\dot{P}_P$ evaluated for the input $U_{M_j}$. The model of Eqn. (9) rewrites then as

$$\dot{X} = \quad F_{M_j}(X) \quad j = 1, \dots, 7. \tag{10}$$

The seven modes of Eqn. (5) can be used to produce the piston movements (positive and negative direction) or to keep its current position (no movement) using three different schemes (or operating configurations).

- Scheme 1 (three-mode configuration): It uses modes 1, 6 and 7 to produce the piston movements such that: mode 1 for no movement, mode 6 for movement in the positive direction and mode 7 for movement in the negative direction.
- Scheme 2 (five-mode configuration): It uses modes 1, 2, 5, 6 and 7 to produce the piston movements such that: mode 1 for no movement, modes 2 and 6 for movement in the positive direction and modes 5 and 7 for movement in the negative direction.
- Scheme 3 (seven-mode configuration): it uses all the modes to achieve no movements and movements in both directions.

As Scheme 3 has more operating modes, the resulting averaged model will be more accurate compared to those obtained from Scheme 2 and Scheme 1. Therefore, if we use the seven-mode averaged model to design a position controller, the tracking error will be small compared to the tracking error resulting when using controllers obtained from Scheme 2 and Scheme 1. However, the implementation of the resulting controller (obtained from the seven-mode model) will be laborious due to the model high complexity. The same arguments are valid when comparing Scheme 2 and Scheme 1. Therefore, to facilitate the position control design, we will consider Scheme 1 with its three basic modes. Note that with a high PWM switching frequency, those basic modes are sufficient to represent the behavior of the switched system as will be illustrated later in this section.

Following the approach of Section 3, we define

$$\begin{pmatrix} x_{1a} \\ x_{2a} \\ x_{3a} \\ x_{4a} \end{pmatrix} = \begin{pmatrix} y_a \\ \dot{y}_a \\ \ddot{y}_a \\ P_{P_a} \end{pmatrix}$$

where $y_a$, $\dot{y}_a$, $\ddot{y}_a$ and $P_{P_a}$ are the averaged position, the averaged velocity, the averaged acceleration and the averaged pressure in chamber $P$. After considering $y_a$ as the output, the three-mode averaged model corresponding to the model of Eqn. (10) is given by

$$\begin{cases} \dot{X}_a = \displaystyle\sum_j d_{M_j} F_{M_j}(X_a) \qquad j \in \{1, 6, 7\} \\ W_a = x_{1_a} \end{cases} \tag{11}$$

with $X_a = (x_{1a}\ x_{2a}\ x_{3a}\ x_{4a})^T$.

The model of Eqn. (11) has three continuous inputs: $d_{M_1}$, $d_{M_6}$ and $d_{M_7}$ with $d_{M_1} + d_{M_6} + d_{M_7} = 1$. As our control objective is to design a robust controller ensuring that the actuator position tracks a desired posi-

tion $y_d$ and in order to be able to apply single-input single-output (SISO), we are interested in transforming the previous model with three continuous inputs into a model with one continuous input. For this purpose, the previous three modes can be merged depending on the movement direction as follows.

- For a movement in the negative direction, that is from chamber $N$ to chamber $P$ (see Fig. 1), the modes 1 and 7 can be modulated together while mode 6 is not used.
- For a movement in the positive direction, that is from chamber $P$ to chamber $N$ (see Fig. 1), the modes 1 and 6 can be modulated together while mode 7 is not used.

To take into account the previous movement direction-based merging, we introduce a new continuous input $u$ such that

- no actuation, that is mode 1 corresponding to $u = 0$;
- full actuation in the positive direction, that is mode 6 corresponding to $u = 1$;
- full actuation in the negative direction, that is mode 7 corresponding to $u = -1$.

and the merging of modes 1, 6 and 7 is as follows.

- For a movement in the negative direction, mode 6 is not used. The input $u$ is negative and its absolute value corresponds to the duty ratio of mode 7 while the duty ratio of mode 1 is the complementary mode, that is

$$\begin{cases} d_{M_1} = 1 - |u| \\ d_{M_6} = 0 \\ d_{M_7} = |u| \end{cases} \qquad u \in [-1, 0[ \qquad (12)$$

- For a movement in the positive direction, mode 7 is not used. The input $u$ is positive and its absolute value corresponds to the duty ratio of mode 6 while the duty ratio of mode 1 is the complementary mode, that is

$$\begin{cases} d_{M_1} = 1 - |u| \\ d_{M_6} = |u| \\ d_{M_7} = 0 \end{cases} \qquad u \in [0, 1] \qquad (13)$$

The model averaging the three-basic modes (mode 1, 6 and 7) with one continuous input is thus given by

$$\dot{X}_a = F_{M_1}(X_a) + \ldots \\ \ldots + \begin{cases} (F_{M_1}(X_a) - F_{M_7}(X_a))u, & u \in [-1, 0[ \\ (F_{M_6}(X_a) - F_{M_1}(X_a))u, & u \in [0, 1] \end{cases} \qquad (14)$$

By considering the averaged position as the output, the state averaged model of (11) becomes

$$\begin{cases} \dot{X}_a = \begin{pmatrix} A_1 & 0 \\ 0 & A_2 \end{pmatrix} X_a + \begin{pmatrix} 0 \\ 0 \\ \varphi_1(X_a) \\ \varphi_2(X_a) \end{pmatrix} + \begin{pmatrix} 0 \\ 0 \\ g_1(X_a) \\ g_2(X_a) \end{pmatrix} u \\ W_a = x_{1_a} \end{cases} \qquad (15)$$

with $u \in [-1, 1]$ and

$$A_1 = \begin{pmatrix} 0 & 1 & 0 \\ 0 & 0 & 1 \\ 0 & 0 & 0 \end{pmatrix} \qquad A_2 = 0$$

$$\varphi_1(X_a) = -\frac{k}{m}\left(\frac{A_P x_{4_a}}{l/2 + x_{1_a}} + \frac{A_N \psi(X_a)}{l/2 - x_{1_a}}\right) x_{2_a} - \frac{b_v}{m} x_{3_a}$$

$$g_1(X_a) = \frac{krT}{m} \begin{cases} \left(\frac{Q(P_S, x_{4_a})}{(l/2 + x_{1_a})} + \frac{Q(\psi(X_a), P_E)}{(l/2 - x_{1_a})}\right) & u \geq 0 \\ \left(\frac{Q(x_{4_a}, P_E)}{(l/2 + x_{1_a})} + \frac{Q(P_S, \psi(X_a))}{(l/2 - x_{1_a})}\right) & u < 0 \end{cases}$$

$$\varphi_2(X_a) = -k \frac{x_{4_a}}{l/2 + x_{1_a}} x_{2_a}$$

$$g_2(X_a) = krT \begin{cases} krT \dfrac{Q(x_{4_a}, P_E)}{(l/2 + x_{1_a}) A_P} \text{ if } u \geq 0 \\ krT \dfrac{Q(P_S, x_{4_a})}{(l/2 + x_{1_a}) A_P} \text{ if } u < 0 \end{cases}$$

and $\psi(X_a) = (A_p x_{4_a} - m x_{3_a} - b_v x_{2_a})/A_N$.

**Remark 2.** *In contrast with the switched model of Eqn. (4) with four binary discrete inputs, the averaged model of Eqn. (15) has the advantage of using only one continuous input $u \in [-1, 1]$. Furthermore, the dynamics $g_1(X_a)$ and $g_2(X_a)$ correspond to the variation of actuation between $F_{M_6}(X_a)$ and $F_{M_7}(X_a)$, which is performed gradually and smoothly contrary to the switched model of Eqn. (4). This behavior is similar to a pneumatic actuator equipped with servo valves where a part of the dynamics of Eqn. (15) depends on the sign of the input $u$: if $u \geq 0$, chamber $P$ is charging while chamber $N$ is discharging and vice versa.*

### 4.2 Analysis of the averaged state model

The use of the averaged model is justified by the high-switching frequency of the solenoid valves. In other

words, the dynamics of these valves are much faster (2 ms according to the data sheets) than the other dynamics of the model. Since the PWM period determines the switching events of the valves, the validity of the averaged model is directly affected by the PWM period. For this reason, the switched model of Eqn. (4) and the averaged state model of Eqn. (15) are compared using their respective outputs $y$ and $y_a$.

Since the closed-loop ensures some robustness against the variation of the PWM period, the comparison will be carried out in an open-loop configuration using an excitation signal. Nevertheless, as there are integrators in its open loop, the system is unstable as any bounded input will result in an unbounded output. Therefore, this excitation input must be well chosen. Keeping in mind that we are operating in an open-loop configuration, this signal must have a relatively small amplitude for the two outputs not to reach the actuator position limits $+l/$ and $-l/2$. Moreover, this signal must result in movements in both directions (positive and negative) to excite the different modes used in each movement. For these reasons, the chosen input is a sinusoidal signal with 10 mm amplitude and 10 Hz frequency.

To compare the averaged model and the switched model, we consider the normalized root-mean-square-output difference (NRMSOD) given by

$$\text{NRMSOD} = \frac{1}{\bar{e}_d}\sqrt{e_d^T e_d} \tag{16}$$

where $e_d = y - y_a$ with $y$ and $y_a$ being the positions in the switched model and the averaged model respectively and $\bar{e}_d$ being the maximal value of $e_d$.

Fig. 5 shows the NRMSOD for different PWM frequencies. The NRMSOD of Eqn. (16) tends toward zero when the PWM frequency increases. Therefore, a high switching frequency such as 100 Hz is sufficient to obtain an averaged model close enough to the switched model with a NRMSD that can be neglected: for a frequency of 100 Hz, this error is around $1\%$ despite that the averaged model uses three modes instead of seven modes as in the switched model.

## 5 SLIDING MODE CONTROL OF THE PNEUMATIC ACTUATOR

In this section, we develop a position controller for our pneumatic actuator. The control strategy aims to make the piston position $y$ tracks a desired sinusoidal trajectory $y_d$ with a sliding mode control strategy as in [19]. Let us define the position tracking error $e_p$ as

$$e_p = x_{1_a} - y_d$$

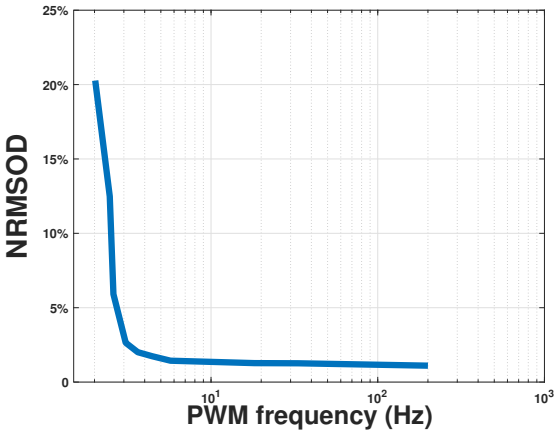


Fig. 5. Normalized root-mean-square-output difference (NRMSOD) vs the PWM frequency

To ensure that the control objective is respected and in order to consider neglected or non-modeled dynamics of the piston[2], a dynamical uncertainty is introduced in the translation dynamic *i.e.* the third dynamics in (15). The new translation dynamic is given by

$$\begin{aligned}\dot{x}_{3_a} = &\left(1 + \Delta_{\varphi_1(X_a)}\right)\varphi_1(X_a) + \dots \\ &\dots + \left(1 + \Delta_{g_1(X_a)}\right) g_1(X_a)\, u\end{aligned} \tag{17}$$

where

$$\left|\Delta_{\varphi_1(X_a)}\right| \leq \gamma \qquad \beta^{-1} \leq \left(1 + \Delta_{g_1(X_a)}\right) \leq \beta$$

with $\gamma > 0$ and $\beta > 1$.

The tracking error $e_p$ converges toward zero asymptotically for any $\Delta_{\varphi_1(X_a)}$ and for any $\Delta_{g_1(X_a)}$ respecting $\left|\Delta_{\varphi_1(X_a)}\right| \leq \gamma$ and $\beta^{-1} \leq \left(1 + \Delta_{g_1(X_a)}\right) \leq \beta$, if the control input $u$ is chosen of the form

$$u = \begin{cases} \dfrac{\widetilde{u} - K_c \text{sign}(s_p)}{\dfrac{krT}{m}\left(\dfrac{Q(P_S, x_{4_a})}{(l/2 + x_{1_a})} + \dfrac{Q(\psi(X_a), P_E)}{(l/2 - x_{1_a})}\right)} & \text{if } \widetilde{u} \geq 0 \\ \dfrac{\widetilde{u} - K_c \text{sign}(s_p)}{\dfrac{krT}{m}\left(\dfrac{Q(x_{4_a}, P_E)}{(l/2 + x_{1_a})} + \dfrac{Q(P_S, \psi(X_a))}{(l/2 - x_{1_a})}\right)} & \text{if } \widetilde{u} < 0 \end{cases} \tag{18}$$

where

- $s_p$ is the sliding surface given by

$$s_p = \left(\frac{d}{dt} + \lambda\right)^3 \int_0^\tau e_p d\tau$$

[2]Such as $f_{ext}$ which was neglected in the model of Eqn. (4).

with $\lambda$ is a positive tuning parameter.

- $\widetilde{u}$ is the control input equivalent to $\dot{s}_p = 0$ and is given by

$$\widetilde{u} = \ddot{y}_d - \varphi_1(X_a) - 3\lambda\ddot{e}_p - 3\lambda^2\dot{e}_p - \lambda^3 e_p \quad (19)$$

- $K_c$ is a time variant gain to ensure some robustness properties and the convergence to the sliding surface, it is given by

$$K_c = \beta\left(\gamma\left|\varphi_1(X_a)\right| + \eta\right) + (\beta - 1)\left|\widetilde{u}\right| \quad (20)$$

with $\eta$ a positive tunning parameter.

**Proof 1.** *See Appendix A.*

## 6 OBSERVABILITY AND OBSERVER DESIGN

### 6.1 Observability analysis of the averaged state model

The observability of a system expresses the possibility to reconstruct its initial conditions with nothing else than the measure of its inputs and outputs. More precisely and as stated in [26–28], a dynamical system is observable if for any two equal outputs $z$ and $\bar{z}$, for any finite time interval $[0, t_h]$, the corresponding initial conditions $x^0$ and $\bar{x}^0$ are also equal. As stated in [26], the previous definition is equivalent to the existence of a state transformation with full rank Jacobian matrix, see [26,27].

In this paper, the averaged state model of Eqn. (15) is already in the canonical form presented in [27] and there is no need for such a transformation. Therefore, the observability proof of the averaged state model of Eqn. (15) will be elaborated as in [28]. For this purpose, two outputs are considered: the averaged position $x_{1_a}$ and the averaged pressure $x_{4_a}$.

Consider two equal output vectors $Z_a = \begin{pmatrix} x_{1_a} & x_{4_a} \end{pmatrix}^T$ and $\bar{Z}_a = \begin{pmatrix} \bar{x}_{1_a} & \bar{x}_{4_a} \end{pmatrix}^T$, that is $x_{1_a} = \bar{x}_{1_a}$ and $x_{4_a} = \bar{x}_{4_a}$. If $x_{1_a} = \bar{x}_{1_a}$ on a finite time interval $[0, t_h]$, we deduce that $x^0_{1_a} = \bar{x}^0_{1_a}$. Since $x_{1_a} = \bar{x}_{1_a}$ their first-time derivatives $x_{2_a}$ and $\bar{x}_{2_a}$ are also equal on $[0, t_h]$ and we conclude that $x^0_{2_a} = \bar{x}^0_{2_a}$. Furthermore, their second-time derivatives $x_{3_a}$ and $\bar{x}_{3_a}$ are also equal on $[0, t_h]$ which means that $x^0_{3_a} = \bar{x}^0_{3_a}$. The same argument applies for $x_{4_a}$ and $\bar{x}_{4_a}$ which leads to $x^0_{4_a} = \bar{x}^0_{4_a}$.

Therefore, for any equal output vectors $Z_a = \begin{pmatrix} x_{1_a} & x_{4_a} \end{pmatrix}$ and $\bar{Z}_a = \begin{pmatrix} \bar{x}_{1_a} & \bar{x}_{4_a} \end{pmatrix}$ the corresponding initial conditions $X^0_a$ and $\bar{X}^0_a$ are equal and the averaged state model of Eqn. (15) is observable using the measures of $x_{1_a}$ and $x_{4_a}$. Furthermore, the averaged state model of Eqn. (15) is uniformly observable since the rank of the Jacobian matrix does not depend on the input $u$.

In the sequel, by considering the output $Z_a = \begin{pmatrix} x_{1_a} & x_{4_a} \end{pmatrix}^T$ the averaged model is given by

$$\begin{cases} \dot{X}_a = \begin{pmatrix} A_1 & 0 \\ 0 & A_2 \end{pmatrix} X_a + \begin{pmatrix} 0 \\ 0 \\ \varphi_1(X_a) \\ \varphi_2(X_a) \end{pmatrix} + \begin{pmatrix} 0 \\ 0 \\ g_1(X_a) \\ g_2(X_a) \end{pmatrix} u \\ Z_a = \begin{pmatrix} C_1 & 0 \\ 0_{1\times 3} & C_2 \end{pmatrix} X_a \end{cases} \quad (21)$$

with $u \in [0, 1]$, $C_1 = (1 \quad 0 \quad 0)$ and $C_2 = 1$.

### 6.2 High-gain observer design

Model of Eqn. (21) is in the canonical form of [27]. Hence, no state transformation is required. A standard high-gain observer can be given by [26, 27]

$$\dot{\widehat{X}}_a = \begin{pmatrix} A_1 & 0 \\ 0 & A_2 \end{pmatrix} \widehat{X}_a + \begin{pmatrix} 0 \\ 0 \\ \varphi_1(\widehat{X}_a) \\ \varphi_2(\widehat{X}_a) \end{pmatrix} + \begin{pmatrix} 0 \\ 0 \\ g_1(\widehat{X}_a) \\ g_2(\widehat{X}_a) \end{pmatrix} u - \ldots$$
$$\ldots - \Theta^{-1} G \left( \begin{pmatrix} C_1 & 0 \\ 0_{1\times 3} & C_2 \end{pmatrix} \widehat{X}_a - Z_a \right) \quad (22)$$

where $u \in [0, 1]$ and

$$\Theta = \begin{pmatrix} \Theta_1 & 0_{3\times 1} \\ 0_{1\times 3} & \Theta_2 \end{pmatrix} \qquad G = \begin{pmatrix} G_1 & 0_{3\times 1} \\ 0_{1\times 3} & G_2 \end{pmatrix}$$

with

$$\Theta_1 = \begin{pmatrix} \theta_1 & 0 & 0 \\ 0 & \theta_1^2 & 0 \\ 0 & 0 & \theta_1^3 \end{pmatrix} \quad \Theta_2 = \theta_2 \quad G_1 = \begin{pmatrix} g_{11} \\ g_{12} \\ g_{13} \end{pmatrix} \quad G_2 = g_2$$

and the parameters $\theta_1$ and $\theta_2$ are strictly positive scalars. The gains in $G_1$ and $G_2$ are chosen such that $A_1 - G_1 C_1$ and $A_2 - G_2 C_2$ are Hurwitz while the parameters $\theta_1$ and $\theta_2$ are chosen sufficiently high to overcome the nonlinear dynamics of the system.

If the different gains are chosen as mentioned above, the observation errors converge toward zero exponentially.

**Proof 2.** *The complete convergence proof can be found in [27].*

### 6.3 Sliding-mode observer design

Given the model of Eqn. (21), we consider the following standard sliding-mode observer [29]

$$\dot{\widehat{X}}_a = \begin{pmatrix} A_1 & 0 \\ 0 & A_2 \end{pmatrix} \widehat{X}_a + \begin{pmatrix} 0 \\ 0 \\ \varphi_1(\widehat{X}_a) \\ \varphi_2(\widehat{X}_a) \end{pmatrix} + \begin{pmatrix} 0 \\ 0 \\ g_1(\widehat{X}_a) \\ g_2(\widehat{X}_a) \end{pmatrix} u - \dots$$
$$\dots - K \left( \begin{pmatrix} C_1 & 0 \\ 0_{1\times 3} & C_2 \end{pmatrix} \widehat{X}_a - Z_a \right) - \dots$$
$$\dots - L \operatorname{sign} \left( \begin{pmatrix} C_1 & 0 \\ 0_{1\times 3} & C_2 \end{pmatrix} \widehat{X}_a - Z_a \right) \tag{23}$$

where $u \in [0, 1]$ and

$$K = \begin{pmatrix} K_1 & 0_{3\times 1} \\ 0_{1\times 3} & K_2 \end{pmatrix} \qquad L = \begin{pmatrix} L_1 & 0_{3\times 1} \\ 0_{1\times 3} & L_2 \end{pmatrix}$$

with

$$K_1 = \begin{pmatrix} k_{11} \\ k_{12} \\ k_{13} \end{pmatrix} \quad K_2 = k_2 \quad L_1 = \begin{pmatrix} \ell_{11} \\ \ell_{12} \\ \ell_{13} \end{pmatrix} \quad L_2 = \ell_2.$$

The gains in $K_1$ and $K_2$ are chosen such that $A_1 - K_1 C_1$ and $A_2 - K_2 C_2$ are Hurwitz.

System of Eqn. (23) is an observer for system of Eqn. (21) where the observation errors converge toward zero asymptotically if $\ell_{11}$, $\ell_{12}$, $\ell_{13}$ and $\ell_2$ satisfy the following conditions

$$\begin{cases} \ell_{11} > \max|e_2| \\ \ell_{12} > 0 \\ -\dfrac{\vartheta - \sqrt{|\zeta|}}{P_3}\ell_{11} < \ell_{13} < -\dfrac{\vartheta + \sqrt{|\zeta|}}{P_3}\ell_{11} \\ \ell_2 > \max|\delta_2| \end{cases} \tag{24}$$

with

$$\zeta = -\frac{4\ell_{12}P_2P_3}{\ell_{11}}\frac{\delta_1}{e_2^2 + e_3^2}e_3, \quad \vartheta = -\big(P_2 + \frac{\delta_1}{e_2^2 + e_3^2}e_2P_3\big)$$

where $P_2$ and $P_3$ are strictly positive scalars. $e_2 = \widehat{x}_{2_a} - x_{2_a}$, $e_3 = \widehat{x}_{3_a} - x_{3_a}$, $\delta_1$ and $\delta_2$ are given by

$$\delta_1 = \varphi_1(\widehat{X}_a) - \varphi_1(X_a) + (g_1(\widehat{X}_a) - g_1(X_a))u$$
$$\delta_2 = \varphi_2(\widehat{X}_a) - \varphi_2(X_a) + (g_2(\widehat{X}_a) - g_2(X_a))u$$

**Proof 3.** *See Appendix B.*

Note that constraints of Eqn. (24) give sufficient conditions on $L$ in order to ensure the observation error convergence toward zero. Those conditions hold even with the switching functions in $g_1(\widehat{X}_a)$ and $g_2(\widehat{X}_a)$. One has to consider the worst-case scenario by considering the worst estimation of $\delta_1$ and $\delta_2$ in both cases ($u \geq 0$ and $u < 0$). Hence, the proof holds for any input $u \in [-1, 1]$ of the averaged model of Eqn. (21).

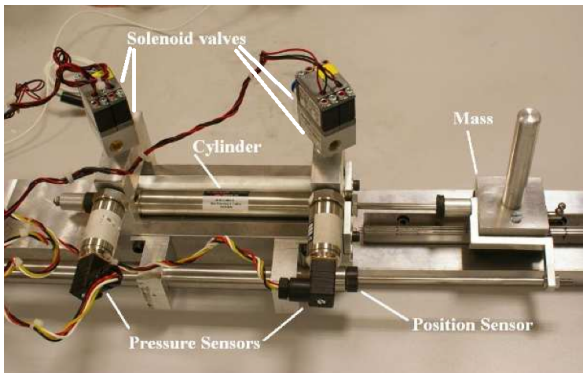


Fig. 6. Pneumatic actuator benchmark

## 7 EXPERIMENTAL RESULTS

The objective of this section is to validate the performance of the designed control input of Eqn. (18) and also the two designed observers of Eqn. (22) and Eqn. (23). These observers are used in closed loop to control the actuator position $y$ using sliding-mode controller to track a desired position $y_d$ given by $0.04\sin(\pi t)$.

### Experimental benchmark characteristics

The solenoid valves[3] used to control the airflow have switching periods of approximately 1.3 ms (opening time) and 0.2 ms (closing time). Therefore, as it was discussed in Section 4.2, with such small-switching periods, the on/off valves are appropriate for control and observation as the resulting averaged model will be accurate enough to represent the switched system.

The controller and the observer are implemented using a dSPACE board (DS1104), running at a sampling rate of 500 Hz. This sampling rate has been chosen according to the open/close bandwidth of the valves and to enable an acceptable tracking response. The benchmark is presented in Fig. 6 and its parameters are summarized in Appendix C.

### Control and observation strategy

The benchmark has three sensors: a position sensor ($y$) and two pressure sensors ($P_P$ and $P_N$). The observers of Eqn. (22) and of Eqn. (23) are used in closed loop with the controller of Eqn. (18) to determine the different inputs $U_i$, see Fig. 7. The observers use the output measures of $y$ and $P_P$ to estimate the averaged state vector $\hat{X}_a$. This latter is injected into a sliding-mode controller to compute the continuous input $u$, which determines the active modes *i.e.* $d_{M_1}$, $d_{M_6}$ and $d_{M_7}$. Finally,

[3] The solenoid valves are GNK821213C3K Matrix models

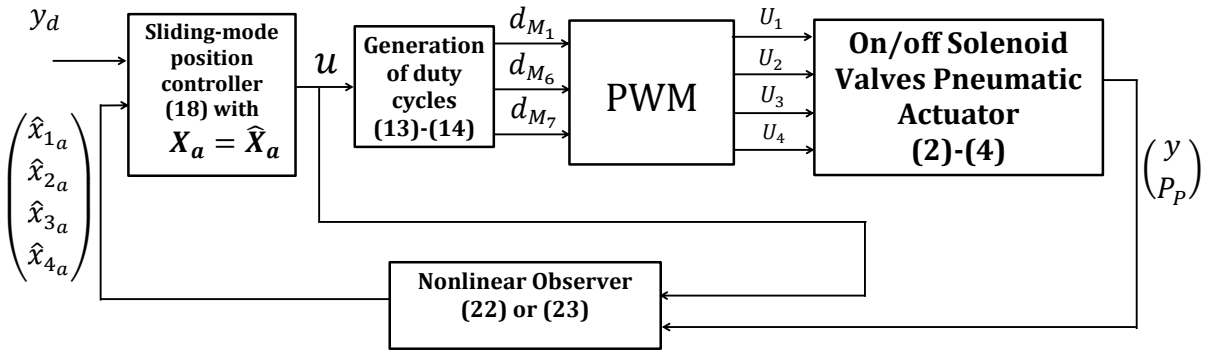


Fig. 7. Observation and control strategy scheme

using a PWM technique for each valve $i$, the different discrete inputs $U_i$ are generated. Note that the measurements of the pressure $P_N$ are not used in the observer or in the control strategy. They are only used to validate the estimation of the pressure $P_N$ given by the observers.

The method used to determine the different control and observation gains can be summarized as follows.

- Step 1: The minimal values ensuring stability are computed using the different theoretical conditions.
- Step 2: starting from the minimal values computed in the first step, simulations are performed, and the gains are adjusted[4] to obtain the desired performance: settling time, overshoot, minimal tracking error.
- Step 3: The computed gains in the second step are used to implement the observer-based controller on the experimental benchmark. Note that minor adjustments may be required to obtain good experimental performance.

Note that in the case of sliding-mode observer, the conditions of Eqn. (24) do not offer a direct method to calculate $L$. The constraints of Eqn. (24) include the observation errors $e_2$ and $e_3$ which are not available. However, in practice, one can use the experimental data to estimate the worst-case estimation of $e_2$ and $e_3$ to satisfy the theoretical constraints.

### 7.1 High-gain observer experimental results

Using the tuning method presented above, the matrices $G$ and $\Theta$ of the observer of Eqn. (22) and the parameters of the sliding mode strategy are the following

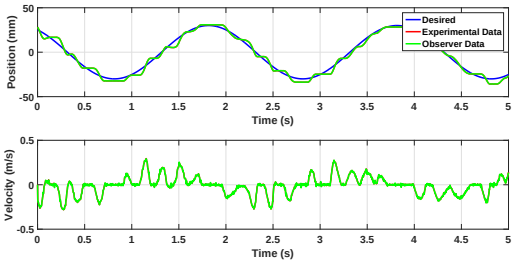


Fig. 8. Actual and estimated position and velocity of the high-gain observer

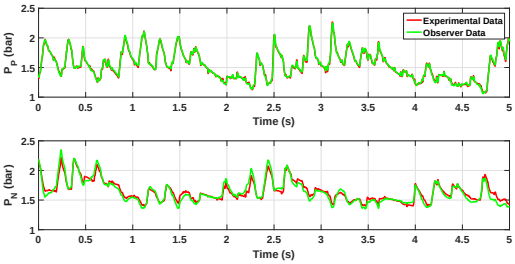


Fig. 9. Actual and estimated pressures of the high-gain observer

$$G = \begin{pmatrix} 150 & 0 \\ 1900 & 0 \\ 10000 & 0 \\ 0 & 30 \end{pmatrix} \qquad \Theta = \begin{pmatrix} 10^2 & 0 & 0 & 0 \\ 0 & 10^4 & 0 & 0 \\ 0 & 0 & 10^6 & 0 \\ 0 & 0 & 0 & 200 \end{pmatrix}$$

$$\lambda = 60 \qquad \beta = 1.1 \qquad \gamma = 0.1 \qquad \eta = 20$$

The experimental results are shown in Fig. 8 and Fig. 9.

[4] Note that the observer gains must ensure that the observation errors converge to zero fast enough for the state estimation to become reliable and to be used by the controller.

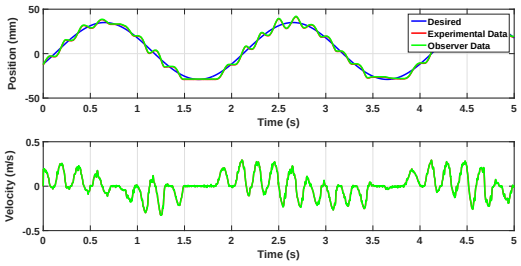


Fig. 10. Actual and estimated position and velocity of the sliding-mode observer

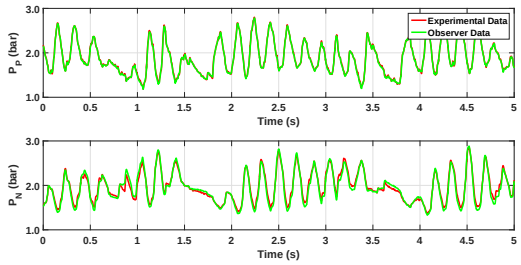


Fig. 11. Actual and estimated pressures of the sliding-mode observer

### 7.2 Sliding-mode observer experimental results

Using the tuning method presented above, the matrices $K$ and $L$ in the observer of Eqn. (23) and the parameters of the sliding mode strategy tuned in practice are as follows

$$K = \begin{pmatrix} 100 & 0 \\ 1840 & 0 \\ 12000 & 0 \\ 0 & 10 \end{pmatrix} \quad L = \begin{pmatrix} 5 & 0 \\ 2 & 0 \\ 15 & 0 \\ 0 & 20 \end{pmatrix} \quad \begin{matrix} \lambda = 60 \;\; \beta = 1.1 \\ \gamma = 0.1 \;\; \eta = 20 \end{matrix}$$

The experimental results are shown in Fig. 10 and Fig. 11.

### 7.3 Discussion

To make a fair comparison of the performances of the two previous observers in a closed loop, the normalized root-mean-square tracking deviation (NRMSTE) is considered as a performance criterion, that is

$$\text{NRMSTE} = \frac{1}{\bar{e}_t}\sqrt{e_t^T e_t} \tag{25}$$

where $e_t = y_d - y$ with $y_d$ and $y$ being the desired position and the benchmark piston position respectively while $\bar{e}_t$ being the maximal value of $e_t$.

In order to ease the comparison, Table. 2 summarizes all the data used in experiments: controller parameters, observer parameters, desired position and the normalized root-mean-square tracking deviation (NRMSTE). For both observers, the NRMSTE of Eqn. (25) is less than 3 % which proves that, despite all the nonlinear phenomena and neglected forces such as $f_{ext}$ in the model of Eqn. (4), the data obtained from observers allows to track the desired position as shown in Fig. 8 and Fig. 10.

Fig. 8 and Fig. 9 show the state estimation of the averaged state variables corresponding to $y$, $\dot{y}$, $P_P$ and $P_N$ using the high-gain observer, while Fig. 10 and Fig. 11 show the state estimation using the sliding-mode observer.

For both observers, the estimations of $y$ and $P_P$ are close to the experimental values. For the estimated velocity $\hat{x}_{2_a}$, it is close to the velocity calculated using a robust differentiation algorithm [30]. For the pressure $P_N$, there is a slight error in the estimation.

Fig. 12 and Fig. 13 show the estimation errors of the high-gain observer and the sliding-mode observer, respectively.

The estimation errors of $y$ do not exceed $0.2$ mm while the velocity estimation error does not exceed $0.03$ m/s for both observers. For the pressures, the estimation error of $P_P$ is less than $0.1$ bar for values reaching 3 bar, which represents less than 3 %. The estimation error of $P_N$ is relatively important and it can reach $0.2$ bar for both observers for values reaching 3 bar, which represents less than 8 %.

Many reasons may be the origin of this relatively important estimation error.

- From an experimental point of view, physical nonlinear phenomena such as dry frictions are present in the physical system. The viscous friction of the cylinder is low, but the global friction of the system is high because of misalignments between the guide rail and the piston/cylinder system: the actuator used in our experiments was attached to a joystick on a rail guide. Another consequence of the dry frictions is the continuous vibrations in the curves of velocity which result in other vibrations in pressure curves. These phenomena can be observed in position curves in Fig. 8 and Fig. 10.
- From a theoretical point of view, the estimated pressure $P_N$ is computed using

$$P_N = \frac{A_P P_P - m\ddot{y} - b_v\dot{y}}{A_N}.$$

This equation is used to compute the estimated pressure $P_N$ presented in Fig. 9 and Fig. 11. This equation was obtained after neglecting the external force

Table 2. Summary of specified data used in experiments

| | high-gain observer | sliding-mode observer |
|---|---|---|
| Observer parameters | $G = \begin{pmatrix} 150 & 0 \\ 1900 & 0 \\ 10000 & 0 \\ 0 & 30 \end{pmatrix}, \Theta = \begin{pmatrix} 10^2 & 0 & 0 & 0 \\ 0 & 10^4 & 0 & 0 \\ 0 & 0 & 10^6 & 0 \\ 0 & 0 & 0 & 200 \end{pmatrix}$ | $K = \begin{pmatrix} 100 & 0 \\ 1840 & 0 \\ 12000 & 0 \\ 0 & 10 \end{pmatrix}, L = \begin{pmatrix} 5 & 0 \\ 2 & 0 \\ 15 & 0 \\ 0 & 20 \end{pmatrix}$ |
| Control parameters | $\lambda = 60 \quad \beta = 1.1$ $\gamma = 0.1 \quad \eta = 20$ | $\lambda = 60 \quad \beta = 1.1$ $\gamma = 0.1 \quad \eta = 20$ |
| Desired trajectory $y_d$ | $0.04 \sin(\pi t)$ | $0.04 \sin(\pi t)$ |
| Normalized root-mean-square tracking error ( NRMSTE) | $2.6417\%$ | $2.7297\%$ |

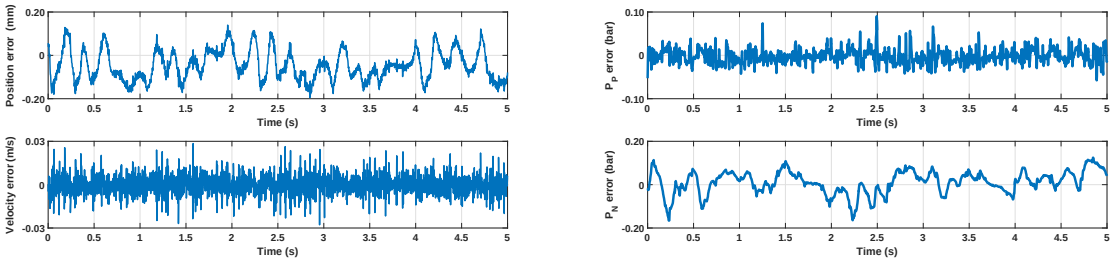


Fig. 12. Estimation errors of the high-gain observer

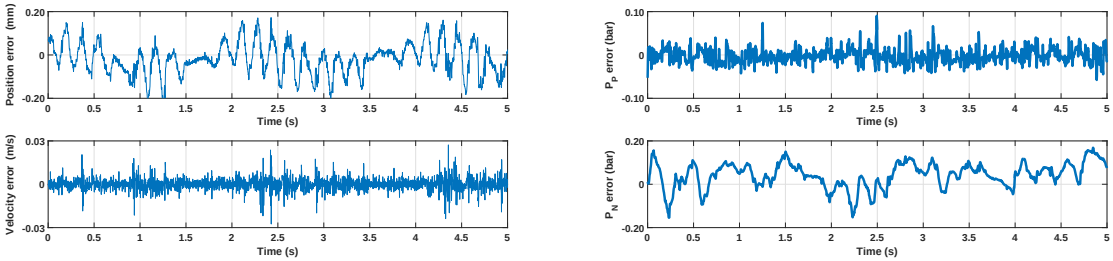


Fig. 13. Estimation errors of the sliding-mode observer

$f_{ext}$ in the translation equation (first equation) of Eqn. (4) and the equation of $P_N$ should be

$$P_N = \frac{A_P P_P - m\ddot{y} - b_v \dot{y} + f_{ext}}{A_N}.$$

Nevertheless, despite all these experimental and theoretical reasons, the estimation of the pressure $P_N$ is good since the estimation error is at most 10 %. These results prove some robustness properties of the designed observers despite that those frictions were not taken into consideration when designing the observers.

## 8 CONCLUSIONS AND PERSPECTIVES

In this paper, we have proposed an averaged state model for a pneumatic actuator equipped with four on/off solenoid valves. The advantage of this approach is to provide a model, which has one continuous input instead of having four binary inputs. This model can easily be used to design control strategies, observers or fault detection strategies. Using this model, we have presented the design of a sliding-mode controller and two nonlinear observers: a high-gain observer and a sliding-mode observer. These observers have been validated experimentally in a closed loop to track the

desired position trajectory. The estimation errors are small, and the trajectory tracking is acceptable.

For the perspectives of this work, various extensions are to be considered. For instance dry frictions were not considered when modeling the system and we have seen that they may affect the experimental performance when it comes to state variable estimation. The consideration of these frictions with appropriate models is our first perspective.

The elaborated model in this paper was obtained using three modes. The elaboration of more complex models with five modes and seven modes to have better performance and to improve the estimation quality is our second perspective.

## REFERENCES


[1] M. Smaoui, X. Brun, and D. Thomasset, "Robust position control of an electropneumatic system using second order sliding mode," *IEEE International Symposium on Industrial Electronics*, vol. 1, no. 5, pp. 905–903, 2006.

[2] M. Smaoui, X. Brun, and D. Thomasset, "Systematic control of an electropneumatic system: Integrator backstepping and sliding mode control," *IEEE Transactions on Control Systems Technology*, vol. 14, no. 5, pp. 905–913, 2006.

[3] M. Yamazaki and S. Yasunobu, "An intelligent control for state-dependent nonlinear actuator and its application to pneumatic servo system," *SICE Annual Conference*, pp. 17–20, 2007.

[4] Y. C. Tsai and A. C. Huang, "Fat-based adaptive control for pneumatic servo systems with mismatched uncertainties," *Mechanical Systems and Signal Processing*, vol. 22, no. 6, pp. 1263–1273, 2008.

[5] M. F. Rahmat, S. N. S. Salim, A. A. M. Faudzi, Z. L. Ismail, S. I. Samsudin, N. H. Sunar, and K. Jusoff, "Non linear modeling et cascade control of an industrial pneumatic actuator system," *Australian Journal of Basic and Applied Sciences*, vol. 5, no. 8, pp. 465–477, 2011.

[6] S. Hajji, A. Ayadi, M. Smaoui, T. Maatoug, M. Farza, and M. M'saad, "Position control of pneumatic system using high gain and backstepping controllers," *Journal of Dynamic Systems, Measurement, and Control*, vol. 141, p. 081001(10), Mar. 2019.

[7] M. Q. Le, M. T. Pham, M. Tavakoli, and R. Moreau, "Development of a hybrid control for a pneumatic teleoperation system using on/off solenoid valves," in *2010 IEEE/RSJ International Conference on Intelligent Robots and Systems*, pp. 5818–5823, Oct. 2010.

[8] K. Pawananont and T. Leephakpreeda, "Sequential control of multichannel on-off valves for linear flow characteristics via averaging pulse width modulation without flow meter: An application for pneumatic valves," *Journal of Dynamic Systems, Measurement, and Control*, vol. 141, p. 011007, Jan. 2019.

[9] E. J. Barth, J. Zhang, and M. Goldfarb, "Control design for relative stability in a PWM-controlled pneumatic system," *Journal of Dynamic Systems, Measurement, and Control*, vol. 125, pp. 504–508, Sept. 2003.

[10] V. Utkine, "Variable structure systems with sliding modes," *IEEE Transactions on Automatic Control*, vol. 22, no. 2, pp. 212–222, 1977.

[11] V. Utkin, J. Gulder, and J. X. Shi, *Sliding Model Control in Electromechanical Systems*. Taylor & Francis Ltd, 1998.

[12] F. Plestan, Y. Shtessel, V. Brġeault, and A. Poznyak, "New methodologies for adaptive sliding mode control," *International Journal of Control*, vol. 83, no. 9, pp. 1907–1919, 2010.

[13] E. Cruz-Zavala, J. A. Moreno, and L. Fridman, "Lyapunov-based design for a class of variable-gain 2nd-sliding controllers with the desired convergence rate," *International Journal of Robust and Nonlinear Control*, vol. 28, no. 17, pp. 5279–5296, 2018.

[14] R. Miranda-Colorado, "Finite-time sliding mode controller for perturbed second-order systems," *ISA Transactions*, vol. 95, pp. 82–92, 2019.

[15] J. Zhang and M. Goldfarb, "Sliding mode approach to PWM-controlled pneumatic systems," *Proceedings on the American Control Conference*, vol. 3, pp. 2362–2367, 2002.

[16] X. Shen, J. Zhang, E. J. Barth, and M. Goldfarb, "Nonlinear averaging applied to the control of pulse width modulated PWM pneumatic systems," *Proceddings of American Control Conference*, vol. 5, pp. 4444–4448, 2004.

[17] X. Shen, J. Zhang, E. J. Barth, and M. Goldfarb, "Nonlinear model-based control of pulse width modulated pneumatic servo systems," *Journal of Dynamic Systems, Measurement, and Control*, vol. 128, pp. 663–669, Nov. 2006.

[18] S. Hodgson, M. Q. Le, M. Tavakoli, and M. T. Pham, "Sliding mode control of nonlinear discrete-input pneumatic actuators," *International Conference on Intelligent Robots and Systems*, pp. 738–743, 2011.

[19] S. Hodgson, M. Tavakoli, M. T. Pham, and A. Lelevé, "Dynamical model averaging and PWM based control for pneumatic actuators," *IEEE International Conference on Robotics and Automation (ICRA)*, pp. 4798–4804, 2014.

[20] R. Prabel, D. Schindele, H. Aschermann, and S. S. Butt, "Model-based control of an electro-pneumatic clutch using a sliding-mode approach," *IEEE Conference on Industrial Electronics and Applications (ICIEA)*, pp. 1195–1200, 2012.

[21] H. Langjord, G. O. Kassa, and T. A. Johansen, "Nonlinear observer and parameter estimation for electropneumatic clutch actuator," *IFAC Symposium on Nonlinear Control Systems*, vol. 8, pp. 789–794, 2010.

[22] H. Langjord, G. O. Kassa, and T. A. Johansen, "Adaptive observer-based switched control for electropneumatic clutch actuator with position sensor," in *IFAC World Congress*, vol. 18, pp. 4791–4796, 2011.

[23] K. Laib, A. R. Meghnous, M. T. Pham, and X. Lin-Shi, "Averaged state model and sliding mode observer for on/off solenoid valve pneumatic actuators," *2016 American Control Conference (ACC)*, pp. 4569–4574, 2016.

[24] T. Takagi and M. Sugeno, "Fuzzy identification of systems and its applications to modeling and control," *IEEE Transactions on Systems, Man and Cybernetics*, vol. 15, no. 1, pp. 116–132, 1985.

[25] K. Tanaka and H. O. Wang, *Fuzzy Control Systems Design and Analysis*. John Wiley & Sons, Inc., 2001.

[26] J. P. Gauthier, H. Hammouri, and S. Othman, "A simple observer for non linear systems applications to bioreactors," *IEEE Transactions on Automatic Control*, vol. 37, no. 6, pp. 875–880, 1992.

[27] G. Besançon and H. Hammouri, "On uniform observation of nonuniformly observable systems," *Systems and Control Letters*, vol. 29, no. 1, pp. 9–19, 1996.

[28] H. Hammouri and M. Farza, "Nonlinear observers for locally uniformly observable systems," *ESAIM: Control, Optimisation and Calculus of Variations*, vol. 9, pp. 353–370, 2003.

[29] C. C. de Wit and J. J. E. Slotine, "Sliding observers for robot manipulators," *Automatica*, vol. 27, no. 5, pp. 859 – 864, 1991.

[30] M. Smaoui, X. Brun, and D. Thomasset, "A robust differentiator-controller design for an electropneumatic system," *Proceedings of the 44$^{th}$ IEEE Conference on Decision and Control, and the European Control Conference*, pp. 4385–4390, 2005.

[31] S. Boyd, L. E. Ghaoui, E. Feron, and V. Balakrishnan, "Linear matrix inequalites in system and control theory," *SIAM Studies in Applied Mathematics*, vol. 15, June 1994.

## APPENDIX

## A TRACKING ERROR ASYMPTOTIC CONVERGENCE PROOF

Consider the closed-loop stability analysis with the following Lyapunov function $V = \frac{1}{2}s_p^2$ which is positive definite. Its time derivative $\dot{V}$ is $\dot{V} = \dot{s}_p s_p$ where $\dot{s}_p$ is given by $\dot{s}_p = \varphi_1(X_a) + g_1(X_a)\,u - \dddot{y}_d + 3\lambda\ddot{e}_p + 3\lambda^2\dot{e}_p + \lambda^3 e_p$. Using Eqn. (17), Eqn. (18) and Eqn. (19), we obtain $\dot{s}_p = -K_c\text{sign}(s_p) + \Delta_{\varphi_1(X_a)}\varphi_1(X_a) + +\Delta_{g_1(X_a)}g_1(X_a)\,u$. Substituting Eqn. (20) in the last expression gives $\dot{s}_p = -\text{sign}(s_p)\Big(\beta\left(\gamma\left|\varphi_1(X_a)\right| + \eta\right) + (\beta-1)\left|\widetilde{u}\right| + \text{sign}(s_p)\Delta_{\varphi_1(X_a)}\varphi_1(X_a) - \text{sign}(s_p)\Delta_{g_1(X_a)}g_1(X_a)\,u\Big)$.

As $|\widetilde{u}| > \text{sign}(s_p)g_1(X_a)u$ and $\beta - 1 > \Delta_{g_1(X_a)}$, it is possible to write $(\beta-1)\left|\widetilde{u}\right| - \text{sign}(s_p)\Delta_{g_1(X_a)}g_1(X_a)\,u > 0$ and $\dot{s}_p$ can be upper bounded by $-\text{sign}(s_p)\left(\beta\Big(\gamma\left|\varphi_1(X_a)\right| + \eta\Big) - \text{sign}(s_p)\Delta_{\varphi_1(X_a)}\varphi_1(X_a)\right)$.
Furthermore, since $\beta > 1$ and $\gamma > \Delta_{\varphi_1(X_a)}$, we obtain $\beta\gamma\left|\varphi_1(X_a)\right| - \text{sign}(s_p)\ \Delta_{\varphi_1(X_a)}\ \varphi_1(X_a) > 0$ and the upper bound of $\dot{s}_p$ becomes $-\beta\ \eta\ \text{sign}(s_p)$. With $\beta > 1$, the previous upper bound becomes $-\eta\ \text{sign}(s_p)$ and the time derivative of the Lyapunov function becomes $\dot{V} < -\eta\left|s_p\right|$ Since $\gamma > 0$, $\dot{V}$ is negative definite. Thus, the tracking error will converge toward zero asymptotically.

## B SLIDING MODE OBSERVATION ERROR ASYMPTOTIC CONVERGENCE PROOF

System Eqn. (21) is observable using two outputs $x_{1_a}$ and $x_{2_a}$ which give two accessible observation errors $e_1 = \widehat{x}_{1_a} - x_{1_a}$ and $e_4 = \widehat{x}_{4_a} - x_{4_a}$. The other errors are $e_2 = \widehat{x}_{2_a} - x_{2_a}$ and $e_3 = \widehat{x}_{3_a} - x_{3_a}$. The error dynamics are given by

$$\begin{cases} \dot{e}_1 = e_2 - K_1 e_1 - \ell_{11}\,\text{sign}(e_1) \\ \dot{e}_2 = e_3 - K_2 e_1 - \ell_{12}\,\text{sign}(e_1) \\ \dot{e}_3 = \delta_1 - K_3 e_1 - \ell_{13}\,\text{sign}(e_1) \\ \dot{e}_4 = \delta_2 - K_4 e_4 - \ell_2\,\text{sign}(e_4) \end{cases} \tag{26}$$

In order to make $e_1$ converges toward zero, one needs to define a sliding surface $s_1 = e_1$ and a Lyapunov function $V_1 = \frac{1}{2}e_1^2$ can be chosen. The convergence of the estimation error to zero is obtained if $\dot{V}_1$ is definite negative. Hence, $\ell_{11}$ must satisfy

$$\begin{cases} \ell_{11} > \;\; e_2 - K_1 e_1 & \text{if} \quad e_1 > 0 \\ \ell_{11} > -e_2 + K_1 e_1 & \text{if} \quad e_1 < 0 \end{cases}$$

Both conditions can be satisfied by estimating the worst-case scenario [28] *i.e.* considering the maximum value of $e_2$ that can occur. Hence, both conditions are satisfied if

$$\ell_{11} > \max|e_2|$$

Then, the sliding surface $s_1$ is attractive and an ideal sliding motion takes place on this surface *i.e.* $e_1 = 0$ and $\dot{e}_1 = 0$. Using Eqn. (26), one can write: $\text{sign}(e_1) = e_2/\ell_{11}$. The error dynamics become

$$\begin{cases} \dot{e}_1 = 0 \\ \dot{e}_2 = e_3 - \ell_{12} e_2/\ell_{11} \\ \dot{e}_3 = \delta_1 - \ell_{13} e_2/\ell_{11} \end{cases}$$

and the dynamics of $e_2$ and $e_3$ can be written as

$$\underbrace{\begin{pmatrix} \dot{e}_2 \\ \dot{e}_3 \end{pmatrix}}_{\dot{e}_{23}} = \underbrace{\begin{pmatrix} -\ell_{12}/\ell_{11} & 1 \\ -\ell_{13}/\ell_{11} & 0 \end{pmatrix}}_{\Lambda} \underbrace{\begin{pmatrix} e_2 \\ e_3 \end{pmatrix}}_{e_{23}} + \underbrace{\begin{pmatrix} 0 \\ \delta_1 \end{pmatrix}}_{\Upsilon}$$

The convergence of $e_{23}$ toward zero is ensured if $\dot{V}_2 < 0$, where $V_2 = e_{23}^T P e_{23}$ and $P = \begin{pmatrix} P_2 & 0 \\ 0 & P_3 \end{pmatrix}$. Recall that $P_2$ and $P_3$ are strictly positive scalars.

The time derivative of $V_2$ is given by

$$\dot{V}_2 = -e_{23}^T \underbrace{\left( -P\Lambda - \Lambda^T P - \frac{e_{23}\Upsilon^T P}{e_{23}^T e_{23}} - \frac{P\Upsilon e_{23}^T}{e_{23}^T e_{23}} \right)}_{M} e_{23}$$

To make $\dot{V}_2 < 0$, one needs to guarantee that $M$ is strictly positive definite where $M$ is given by

$$M = \begin{pmatrix} 2\dfrac{\ell_{12}P_2}{\ell_{11}} & \dfrac{\ell_{13}}{\ell_{11}}P_3 - P_2 - \dfrac{e_2\delta_1 P_3}{e_2^2+e_3^2} \\ P_3\dfrac{\ell_{13}}{\ell_{11}} - P_2 - \dfrac{P_3\delta_1 e_2}{e_2^2+e_3^2} & -2\dfrac{P_3\delta_1 e_3}{e_2^2+e_3^2} \end{pmatrix}$$

Using Schur's Lemma [31], $M$ is positive definite if and only if

$$\begin{cases} 2\dfrac{\ell_{12}P_2}{\ell_{11}} > 0 \\ -4\dfrac{P_3\delta_1 e_3}{e_2^2+e_3^2}\dfrac{\ell_{12}P_2}{\ell_{11}} - \left(\dfrac{\ell_{13}}{\ell_{11}}P_3 - P_2 - \dfrac{e_2\delta_1 P_3}{e_2^2+e_3^2}\right)^2 > 0 \end{cases}$$

Hence, the conditions on $\ell_{12}$ and $\ell_{13}$ given in Eqn. (26) are obtained and the errors $e_2$ and $e_3$ converge toward zero. Finally, for the remaining error $e_4$, similarly to $e_1$, a Lyapunov function $V_4 = \frac{1}{2}e_4^2$ can be defined. In order to make its time derivative $\dot{V}_4$ definite negative, $\ell_2$ must satisfy

$$\begin{cases} \ell_2 > \;\; \delta_2 - K_4 e_4 & \text{if} \quad e_4 > 0 \\ \ell_2 > -\delta_2 + K_4 e_4 & \text{if} \quad e_4 < 0 \end{cases}$$

Both conditions can be satisfied if $\ell_2 > \max|\delta_2|$.

## C BENCHMARK PARAMETERS

The values given in the following table come from the different manufacturer data sheets or an *a priori* estimation of the parameters.

Table 3. Benchmark parameters

| Parameters | Values |
|---|---|
| $m$ | 0.9 kg |
| $b_v$ | 50 N.s.m$^{-1}$ |
| $l$ | 0.01 m |
| $A_P$ | $1.81 \times 10^{-4}$ m$^2$ |
| $A_N$ | $1.81 \times 10^{-4}$ m$^2$ |
| $k$ | 1.2 |
| $r$ | 286.68 J.(kg.K)$^{-1}$ |
| $T$ | 296 K |
| $P_S$ | 3.01 bar |
| $P_E$ | 1.01 bar |
| $b_{crit}$ | 0.493 |
| $C_{val}$ | $3.4 \times 10^{-9}$ kg.(s.Pa)$^{-1}$ |